

## RESEARCH ARTICLE

# Recognition of the Shape and Location of Multiple Power Lines Based on Deep Learning With Post-Processing

HYUN-SIK SON<sup>1,3</sup>, DEOK-KEUN KIM<sup>2,3</sup>, SEUNG-HWAN YANG<sup>3</sup>, AND YOUNG-KIU CHOI<sup>1</sup><sup>1</sup>Department of Electrical and Computer Engineering, Pusan National University, Geumjeong-gu, Busan 46241, Republic of Korea<sup>2</sup>Interdisciplinary Program in Agricultural and Life Science, Chonnam National University, Buk-gu, Gwangju 61186, Republic of Korea<sup>3</sup>Smart Agricultural Machinery Research and Development Group, Korea Institute of Industrial Technology, Gimje-si, Jeollabuk-do 54325, Republic of Korea

Corresponding authors: Seung-Hwan Yang (yangsh@kitech.re.kr) and Young-Kiu Choi (ykichoi@pusan.ac.kr)

This work was supported by the Korea Institute of Planning and Evaluation for Technology in Food, Agriculture and Forestry (IPET) and the Korea Smart Farm Research and Development Foundation (KosFarm) through the Smart Farm Innovation Technology Development Program, funded by the Ministry of Agriculture, Food and Rural Affairs (MAFRA) and the Ministry of Science and ICT (MSIT), Rural Development Administration (RDA) under Grant 421032-04.

**ABSTRACT** Power line collisions pose a significant threat to the safety of drones. This is because it is difficult for drone pilots to recognize power lines at long distances, even on sunny days, and power lines are less visible in rainy or foggy weather. Therefore, power line detection is necessary for safe drone flight. This article proposes an algorithm that can recognize various shapes and locations of multiple power lines while improving the recognition performance of power lines compared to previous studies. YOLO, a deep learning technology used for object detection, is used to recognize power lines as multiple bounding boxes, and center points of these bounding boxes are sorted and integrated. This algorithm improves the power line detection performance by excluding incorrectly detected power lines and restoring undetected parts of the power lines. The performance of the proposed method was evaluated using the intersection-over-union (IoU) and F1-score, which were 0.674 and 0.528, respectively. This performance was superior to those of U-Net, LaneNet and BiSeNet V2 which are deep learning technologies for segmentation. The proposed method was mounted on the embedded system of the test drone, and tests were conducted indoor and outdoor. Then, the average frames per second (FPS) value was calculated as 10.05. Various shapes and locations of multiple power lines can be recognized in real-time using the power line recognition method proposed in this paper.

**INDEX TERMS** Power line detection, continuous object, segmentation, agricultural spraying drone, unmanned aerial vehicle (UAV).

## I. INTRODUCTION

With technological advancements, drones are being used in various fields, such as military, disaster relief, traffic observation, and agriculture. Recent studies on drones have focused on obstacle detection and collision avoidance [1], [2], [3]. Power lines are among the most dangerous obstacles for drone flight. When a drone is far from its pilot, it is difficult for the pilot to identify the power line, which increases the risk of drone collision. Therefore, power line

collision accidents are increasingly threatening the safe flight of drones.

In recent years, several techniques have been proposed for detecting power lines. Power line detection using the traditional image processing technology method detects the edge map of the image and the power line using the Hough transform or line trace algorithm [4], [5], [6]. However, with the development of deep learning methods, recent studies have been conducted to detect power lines using convolutional neural networks (CNNs). Traditional image processing requires manual design of power line features, but deep learning can automatically train the features. Therefore, deep learning can maintain higher recognition accuracy

The associate editor coordinating the review of this manuscript and approving it for publication was Halil Ersin Soken.

in various environments than traditional image processing. A study on power line detection has used a method of constructing learning data using a physically based rendering approach. For the deep learning of power lines, a model with a custom version of the VGG-16 network as the backbone was used [7]. The other study used networks such as U-Net, SegNet, and PSPNet to learn power lines. Their learning data were composed only of images with power lines. Semantic segmentation was performed using a CNN on multispectral images obtained from an unmanned aerial vehicle (UAV) [8]. However, the detection of curved power lines has not yet been attempted. A fast power line detection network (fast-PLDN), which is a real-time semantic segmentation model, detects straight and curved power lines based on a pixel-by-pixel. To improve the power line detection results along the boundary, a network with low-high-pass blocks and edge-attention fusion modules that effectively extract spatial and semantic information was used. It recognized a curved power line, but the curvature was gentle [9]. Most studies using deep learning for conventional power line detection have been conducted using GPU computers for high performance. In a previous study for the embedded system, tiny YOLOv3 using the multiple bounding box method was used to detect power lines. This method is trained by labeling continuous objects with multiple bounding boxes, at which the mean Average Precision (mAP) was evaluated to be 94.00, and the frames per second (FPS) value was 12.5 [10].

The main contributions of this study are as follows.

- 1) Segmented power line detection (SPLD), applying a post-processing algorithm to the multiple bounding box method using deep learning for the power line detection, is proposed. The SPLD improves the power line detection performance by excluding incorrectly detected power lines and restoring undetected parts of the power lines.
- 2) Through the SPLD, the shape and location of power lines can be known simultaneously.
- 3) The SPLD can recognize not only horizontal power lines but also diagonal and curved power lines, and inform the number of power lines in images.

This study has been conducted to recognize power lines using deep learning for agricultural spraying drones. To attach it to the drone, an embedded computer with low weight and power consumption was required. Therefore, Jetson Nano was used as the embedded computer, and the YOLOv5s model was used as the deep learning technology suitable for embedded computers [11]. YOLOv5 has been utilized in various fields, such as the detection of kiwifruit defects [12], boulders from planetary images [13], and fabric defects [14]. The performance of power line recognition using the SPLD was evaluated by the intersection over union (IoU) and F1-score. Additionally, the IoU and F1-score were compared with them through LaneNet, U-Net and BiSeNet V2, which are deep learning models that use semantic segmentation.

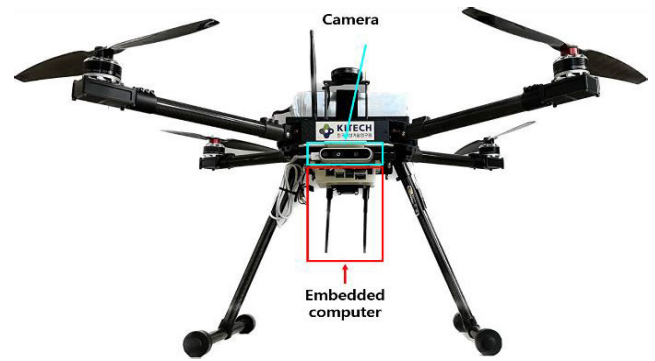


**FIGURE 1.** Test drone equipped with the embedded computer and camera for the SPLD.

LaneNet [15], [16], [17] and U-Net [18], [19], [20], [21] have been used to recognize lines, such as lanes and power lines. BiSeNet V2 [22] demonstrates high model performance while having a fast inference speed. Finally, the SPLD was mounted on the embedded system of the test drone. Tests for power line recognition were conducted indoors and outdoors.

## II. METHODS

### A. EXPERIMENTAL PROCEDURE

The training and test images of power lines used in deep learning were obtained directly through drone flight, and 399 and 35 images, respectively, were used. The images contained more than one power line; the images used for training contained 1146 power lines, and the images used for testing contained 78 power lines. The performance of the SPLD was compared with learning the same data through the U-Net, LaneNet and BiSeNet V2. Their performance was evaluated using the IoU and F1-score, which are commonly used for performance evaluation in semantic segmentation. The IoU evaluates the performance by determining how well the predicted value overlaps with the actual value, and the F1-score evaluates the performance using the harmonic average of precision and recall.

Also, indoor and outdoor tests were conducted using a test drone equipped with an embedded computer, as shown in Fig. 1. The specifications of the test drone and the embedded systems are listed in Table 1. An indoor experiment was conducted with a virtual environment. In the virtual environment, two power lines with a thickness of 3 mm were installed against the paddy field image as the background, and the test drone was placed at a distance of 1 m. An outdoor experiment was conducted using the test drone in a paddy field located in Gimje-si, Jeollabuk-do. The test drone flew within 5–10 m from the power line and detected the power line.

### B. SEGMENTATION OF POWER LINES

#### 1) YOLOV5

In this study, YOLOv5 was used as the deep learning model for power line learning and detection. The structure of YOLOv5 consists of three parts: a backbone that extracts

**TABLE 1. Specifications of the test drone and embedded systems.**

Item	Specification
Drone dimensions	975 × 975 × 430 mm (width × length × depth)
Drone weight	6.15 kg
Embedded computer	NVIDIA Jetson Nano
Embedded computer OS	Ubuntu 18.04 LTS
GPU accelerated library	CUDA 10.1 and CUDNN 7.6.5
Camera	Intel RealSense D435i

features, a neck that improves performance by fusing the extracted features, and a head that converts features into bounding box parameters. The backbone is a CNN that extracts feature maps of various sizes from the input images through multiple convolutional and pooling layers. Convolution with batch normalization and leaky-ReLU (CBL), cross-stage partial (CSP), and spatial pyramid pooling (SPP) techniques were used. CBL is a block composed of a convolutional layer, batch normalization, and leaky-ReLU activation function, and is used to extract features. CSP performs a convolution operation on only one part of a feature map and integrates it with the rest of the feature map. As only some of the feature maps pass through the convolutional layer, the amount of computation can be reduced, and the flow of the gradient can be efficiently performed in the backpropagation process, which can improve performance. SPP improves the performance by max pooling feature maps with filters of various sizes and then merging them again. In the neck part, feature maps of various sizes are fused. A path aggregation network is used to fuse low- and high-level features to improve performance. The head converts the feature output from the neck into the network's final output using a convolution layer. The final output of the network includes the bounding box parameters, the probability that an object exists with, and the probability that a class exists with. YOLOv5 is divided into YOLOv5s, YOLOv5m, YOLOv5l, and YOLOv5x. The performance of the model improves as one goes from s to x, but the processing time increases [11]. In this study, the YOLOv5s model was used because of the performance limitations of the embedded computer.

## 2) LEARNING POWER LINES USING YOLOV5

A power line is not a single object with clear boundaries, such as a car, tree, or animal, but rather a continuous object with unclear boundaries. Therefore, it is inappropriate to use learning data based on existing labeling methods. Labeling for power line learning was performed with several bounding boxes, whose size was 0.05 times the size of the image. This bounding box size has been shown to be optimal for power line detection in a previous study [10]. The size and labeling

**FIGURE 2. Labeling using a bounding box of size 0.05 times the size of the image.****TABLE 2. Specifications of the deep learning computer for learning.**

Item	Specification
CPU	Intel Core i7-7700K 4.20 GHz
GPU	NVIDIA GTX 2080 Ti
RAM	32 GB
OS	Ubuntu 18.04 LTS
Program	Python3.6
GPU accelerated library	CUDA 10.1 and CUDNN 7.6.5

**TABLE 3. Hyperparameters for training power lines.**

Parameter	Value
Momentum	0.9738
Learning rate	0.0081
Decay	0.0005
Iteration	100000

method of the bounding box of the power line for learning are shown in Fig. 2. A total of 22,315 power line labeling procedures were performed using 399 learning data. The training image size was 416 × 416 pixel, then the bounding box size was 21 × 21 pixel. The specifications of the computer used for learning are listed in Table 2. The hyperparameters for training the YOLOv5 are listed in Table 3. To find optimal hyperparameters, the Hyperparameter Evolution library was used [11]

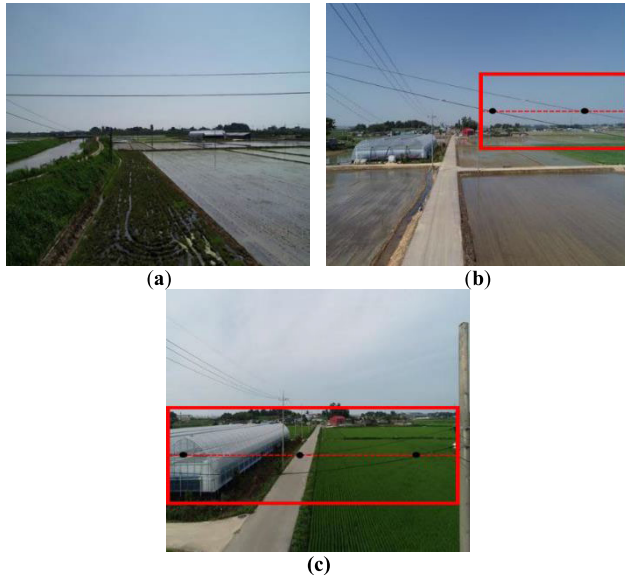


FIGURE 3. (a) horizontal power lines (b) diagonal power lines (c) curved power lines.

### 3) POST-PROCESSING ALGORITHM FOR POWER LINE SEGMENTATION

Power lines were recognized with multiple bounding boxes, and they were segmented through a post-processing algorithm. If there is only one power line in the image, it is simply integrated by connecting the detected bounding boxes. However, if there are multiple power lines in an image, multiple bounding boxes are randomly detected, making it difficult to classify the power lines individually. Therefore, a post-processing algorithm is needed to classify and integrate the detected bounding boxes. The power line can appear in three major shapes, as shown in Fig. 3. When the shapes of all power lines are horizontal, as shown in Fig. 3a, a segmentation of the power lines can indicate that the bounding boxes existing on the same horizontal line among the center points of the detected bounding boxes are the same. However, if they are diagonal or curved, as shown in Fig. 3b and 4c, there are cases where there are two power lines on the same horizontal line, such as the black dot in the red box. To solve this problem, the power lines were segmented according to the flowchart in Fig. 4. First, the x- and y-axis pixel values are extracted from the center points of several bounding boxes where the power line is detected based on the image pixel, and these points are sorted in ascending order based on the x value. The first point among the sorted center points becomes the first center point of the power line in the image. The second center point becomes the next center point of the same power line as the first center point if the difference in y value between the first and second center points is smaller than the set threshold, and if it is larger, it becomes the first center point of another power line. The third center point is determined whether it is a new power line or the next center point of a previously recognized power line by comparing the difference in y values with the previous center points.

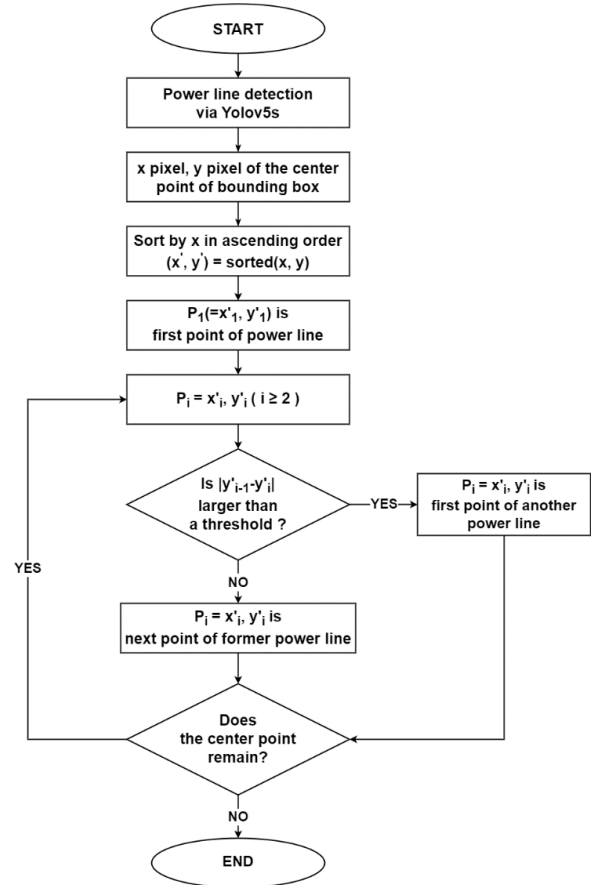
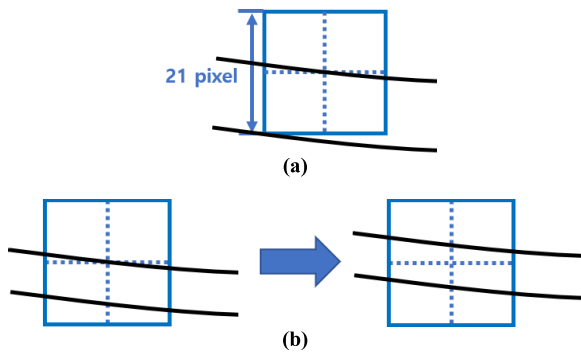


FIGURE 4. Flowchart of the SPLD.

In this study, a threshold of 10 pixels was set based on the size of the bounding box during labeling. As illustrated in Fig. 5a, a bounding box is labeled per power line when the pixel difference between two adjacent power lines on the y-axis is greater than 10 pixels. If the pixel difference is less than 10 pixels, the bounding box would overlap with other power lines. In such cases, the two adjacent power lines are labeled as a single bounding box, as shown in Fig. 5b. By repeating this method, several power lines in the image could be recognized individually. In order to correct the deep learning detection error, power lines composed of 5 or fewer center points are considered not to be power lines.

For example, if two power lines are detected as shown in Fig. 6a, the center points of the bounding boxes of the detected power lines are sorted in the order of  $P_1, P_2, P_3, P_4, P_5, P_6, P_7, P_8$ . Among the sorted center points, the first center point  $P_1$  becomes the first center point of power line B. When  $P_1$  and  $P_2$  are compared, the difference between their y values,  $\Delta y$ , is larger than the set threshold; therefore,  $P_2$  is treated as a different power line from  $P_1$ , and then  $P_2$  becomes the first center point of power line A. The difference in y value between  $P_3$  and  $P_1$  is larger than the set threshold, but one between  $P_3$  and  $P_2$  is within the set threshold. Therefore,  $P_3$  is segmented into the second center point of power line A. In addition, because the center points are rarely accurately



**FIGURE 5.** (a) the case where the difference between the two power lines is more than 10 pixels (b) the case where the difference between the two power lines is less than 10 pixels.

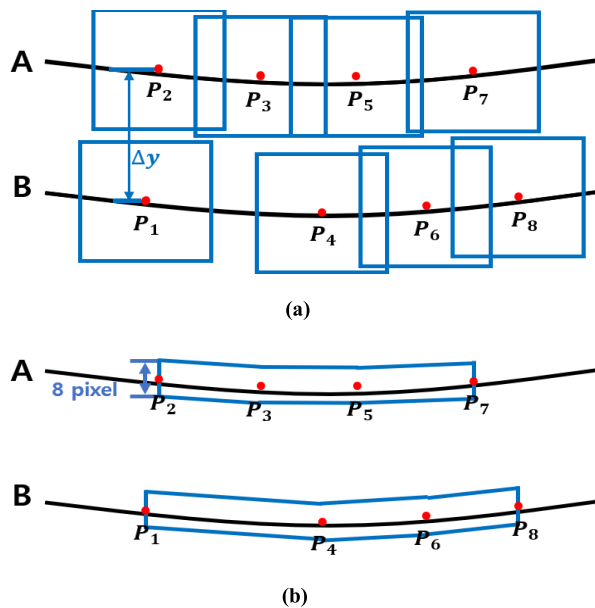


**FIGURE 6.** (a) Result of power line recognition through YOLOv5s using multiple bounding box method (b) Result of power line recognition using the SPLD.

located on the power line, the area of the power line is assumed to be 4 pixels above and below the center point. Finally, individual areas of power lines A and B are detected by connecting each point above and below the center points as shown in Fig. 6b.

### C. DEEP LEARNING USING SEGMENTATION

#### 1) LANENET

In this study, the performance of the proposed the SPLD method was compared with that of LaneNet. The architecture of LaneNet is shown in Fig. 7. The LaneNet treats lane detection as an instance segmentation problem and trains it as an end-to-end system. It can handle lane changes without being limited by the number of lanes that the network can detect. The LaneNet consists of a segmentation branch and an embedding branch. The segmentation branch is trained to output a binary segmentation map that indicates the pixels that belong to a lane. To construct the ground-truth

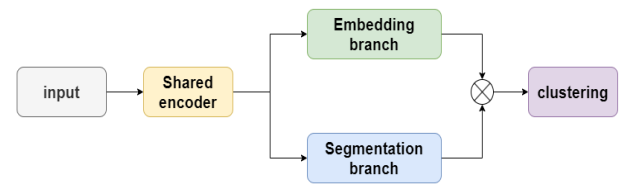


**FIGURE 7.** LaneNet architecture.

segmentation map, the points of all ground-truth lanes are connected to form a connected line per lane. Ground-truth lanes are drawn even if they are covered by cars or do not have explicit visual lane segments, such as dotted or faded lanes. The position of a lane is learned to be predicted even when it is covered. The embedding branch is trained using a one-shot method based on distance measurement learning to classify the next-best pixels identified by the segmentation branch. Using the clustering loss function, the embedding branch is trained to output embeddings for pixels in each lane such that the distance between pixel embeddings belonging to the same lane is short, whereas the distance between pixel embeddings belonging to different lanes is large. Pixel embeddings in the same lane are clustered together to form a unique cluster per lane. The LaneNet is being studied for lane departure for autonomous vehicles or lane detection for trajectory planning decisions [15], [16], [17].

#### 2) U-NET

In this study, the performance of the proposed the SPLD method was compared with that of the U-Net. It consists of a contracting path (left) and an expanding path (right). The contracting path has the general structure of a convolutional network. It consists of repeatedly applying two  $3 \times 3$  convolutions (unpadded convolutions), followed by a  $2 \times 2$  max pooling operation, each using a ReLU and stride for downsampling. At each downsampling step, the number of channels in the feature map is doubled. Every step in the expanding path consists of upsampling the feature maps, a  $2 \times 2$  convolution that halves the number of channels in the feature maps, and a  $3 \times 3$  convolution and ReLU for concatenation with the truncated feature maps in the contracting path. Cropping is necessary because the border pixels are lost in every convolution. In the final layer, a  $1 \times 1$  convolution is used to map the 64-component feature vector to the desired number of classes. The network has 23 convolutional layers. To allow seamless tiling of the output partitioning map, the input tile size needs to be chosen such that all  $2 \times 2$  max pooling operations are applied to layers of even x and y sizes. The U-Net is being studied in areas, such as lane recognition for autonomous vehicles [18], [19], road area extraction for remote sensing [20], and road network information extraction using satellite images [21].

#### 3) BISENET V2

To speed up model inference, current approaches almost always sacrifice low-level details, resulting in significant accuracy reduction. Bilateral Segmentation Network

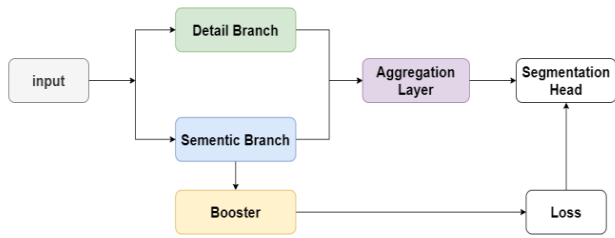


FIGURE 8. BiSeNet V2 architecture.

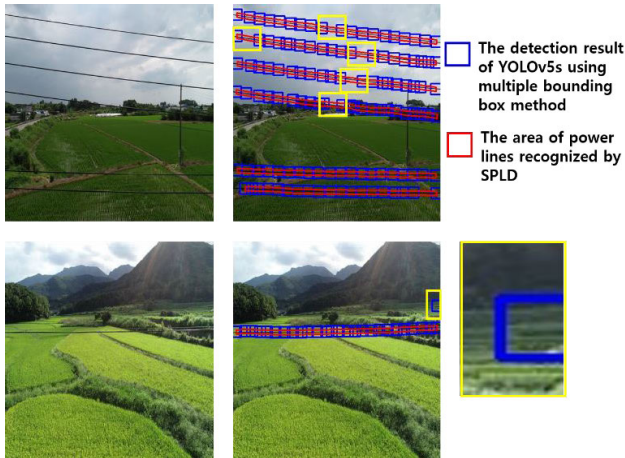


FIGURE 9. Results of power line detection and error correction using the SPLD.

(BiSeNet) V2 handles these spatial details and categorical semantics separately to achieve high accuracy and high efficiency for real-time semantic segmentation. BiSeNet V2 consists of three parts: Detail Branch, Semantic Branch, and Guided Aggregation Layer. The Detail Branch consists of wide channels and shallow layers. These capture low-level details and create high-resolution feature representations. Semantic branches are composed of narrow channels and deep layers to obtain high-level semantic context. Semantic Branches are lightweight because they use reduced channel capacity and fast downsampling. The Guided Aggregation Layer reinforces interconnection and fuses the two types of functional representation. Moreover, booster training strategies are used to improve segmentation performance without additional inference costs. The booster training strategy inserts a segmentation head into a semantic branch in the training phase and discards it in the inference phase [22]. The architecture of BiSeNet V2 is shown in Fig. 8.

### III. EXPERIMENTAL RESULTS

#### A. POWER LINE RECOGNITION

Fig. 7 shows part of the result of recognizing the power line using the SPLD for the test image. The blue box is the detection result of YOLOv5s using the multiple bounding box method, and the red box is the area of power lines recognized by the SPLD. As shown by the yellow box in

the upper image of Fig. 7, the power line bounding boxes detected by YOLOv5s did not recognize some parts of power lines. However, the SPLD result shows that this error was corrected and the entire power line was recognized. In addition, as shown in the yellow box in the lower image, even when YOLOv5s recognizes non-power lines as power lines, the SPLD normally excluded it from recognized power lines.

#### B. PERFORMANCE EVALUATION OF POWER LINE RECOGNITION

Fig. 10 shows examples of five different types of power lines among the 35 test images and the results of recognizing power lines using the U-Net, LaneNet, BiSeNet V2 and SPLD. Image 1 in Fig. 8 shows a case in which there were three power lines on different backgrounds. The U-Net detected only one power line on a light background, while LaneNet detected one on a light background and another on a dark background. However, the SPLD and BiSeNet V2 detected all three power lines. Image 2 shows an example of a short power line in the upper-left corner. The U-Net, LaneNet and BiSeNet V2 recognized the short power line, but the SPLD excluded it from the recognition result because it was composed of 5 or fewer center points. The characteristics of the differences in the detection results of each method can be confirmed in the case where two power lines were closely attached, as shown in Images 3 and 4. The U-Net recognized each power line. In the case of the LaneNet, nearby several power lines were recognized as a thick power line. The Bisenet V2 did not correctly recognize the two adjacent power lines in Image 3. However, in Image 4, two nearby power lines were recognized as one power line. As mentioned in the method section, two power lines within 10 pixels were labeled as one power line to create training data and trained with YOLOv5s. So, as shown in Image 3 and 4, the SPLD recognized the power line to pass through the center of the two power lines. The result obtained using the U-Net shows that the power line was well recognized against a light-colored background, such as the sky. However, the power line was not recognized against a dark background, such as a paddy field or mountain. The results obtained using the LaneNet show that power lines were recognized against both light and dark backgrounds. However, some parts of the power line were not recognized, or the area of the power lines was recognized as thick. BiSeNet V2, SPLD results show that the power line was recognized on both light and dark backgrounds. BiSeNet V2 sometimes incorrectly detected ridges as power lines, but the SPLD did not incorrectly detect ridges as power lines. The SPLD can also provide information about the number of power lines and their location in images.

Table 4 shows the IoU and F1-score of the U-Net, LaneNet, Besenetv2 and the SPLD using 35 test data. It also shows the FPS when power lines are recognized in real-time using an embedded computer. The F1-scores of the U-Net, LaneNet and BiSeNet V2 were 0.431, 0.465 and

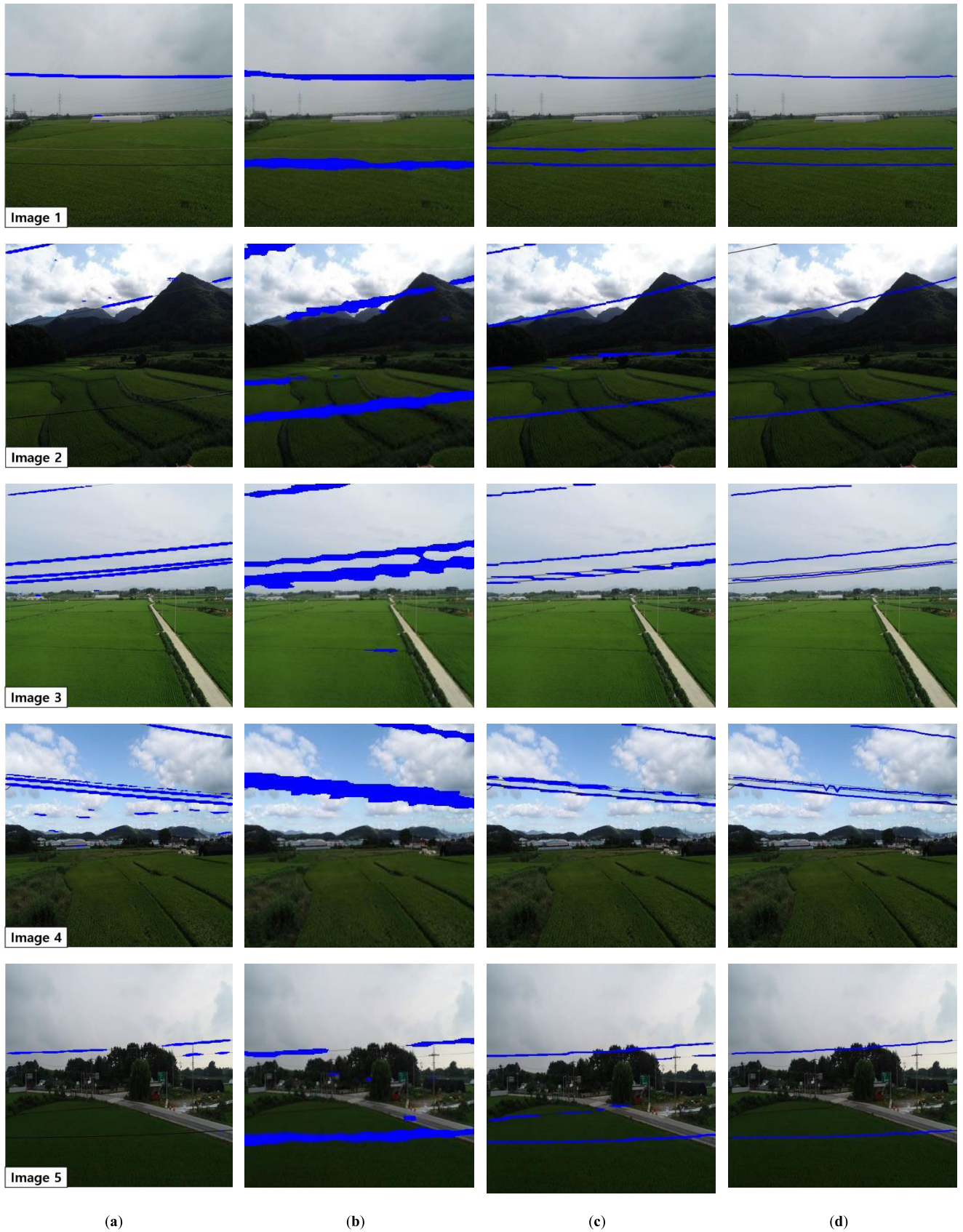


**FIGURE 10.** (a) Power line recognition results using U-Net (b) Power line recognition results using LaneNet (c) Power line recognition results using the BiSeNet V2 (d) Power line recognition results using the SPLD.

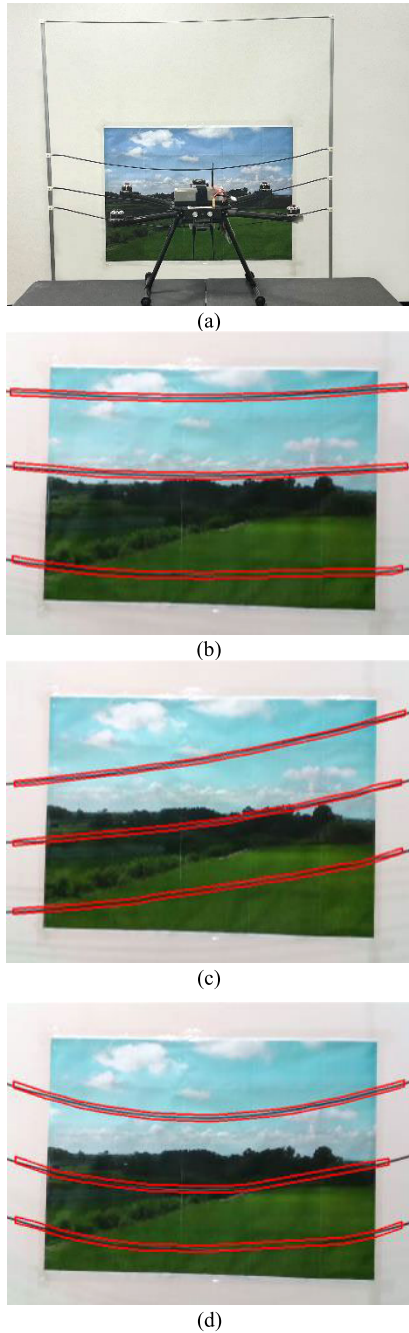


FIGURE 11. (a) Indoor test environment (b) three horizontal power lines (c) three diagonal power lines (d) three curved power lines.

0.663, respectively, and that of the SPLD was 0.674. The IoU of the U-Net, LaneNet and BiSeNet V2 were 0.295, 0.309 and 0.507, respectively, and that of the SPLD was 0.528. The difference in performance is due to the recognition characteristics of the three methods mentioned above. This shows that the SPLD is better suited for recognizing power lines in agricultural environments. Among the studies that evaluated the performance of recognizing lines or objects by deep learning with the IoU and F1-score, when recognizing lanes [17], when recognizing road networks using satellite

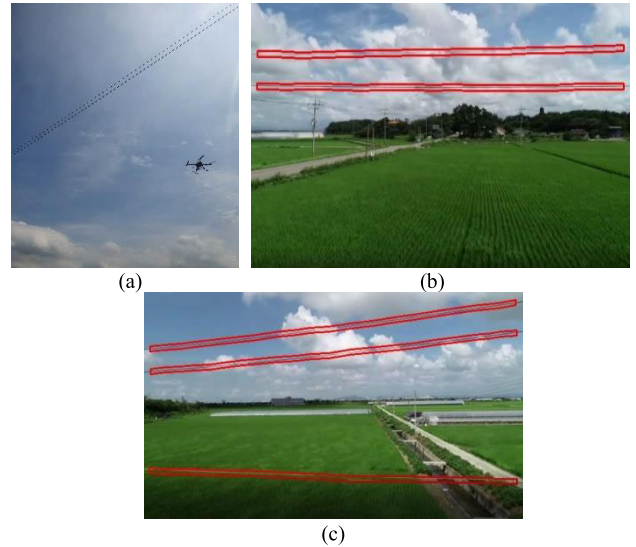


FIGURE 12. (a) Outdoor test environment (b) two horizontal power lines (c) one horizontal power line and two diagonal power lines.

TABLE 4. Power line recognition performance according to deep learning model.

	U-Net	LaneNet	BiSeNet V2	SPLD
F1-score	0.431	0.465	0.663	0.674
IoU	0.295	0.309	0.507	0.528
FPS	0.436	0.015	5.80	10.05

images [21], and when recognizing small objects in urban remote sensing images [23], the IoU was calculated as 0.511–0.651 and the F1-score was calculated as 0.829–0.890. The IoU and F1-score of the SPLD are similar to other studies. The FPS of U-Net, LaneNet, and BiSeNet V2 were 0.436, 0.015, and 5.80, respectively, and the SPLD was 10.05.

C. THE SPLD TEST USING EMBEDDED SYSTEM

Fig. 11a shows indoor virtual environment conditions and the test drone equipped with the embedded system running the SPLD. In this virtual environment, three power lines were set in horizontal, diagonal and curved shapes, and these power lines were successfully recognized as shown in Fig. 11b, 11c and 11d. Fig. 12a shows the test drone detecting power lines in a paddy field in real-time. During a drone flight, the SPLD recognized power lines of various shapes and numbers, and Fig. 12b and 12c show their examples.

IV. CONCLUSION

This study was conducted to develop a power line recognition technology for the safe flight of agricultural spraying drones. The segmented power line detection (SPLD) method was proposed to recognize power lines. The SPLD detects power lines by YOLOv5s using the multiple bounding



box method and recognizes the area of individual power lines by post-processing for power line segmentation. When recognizing multiple power lines using only YOLOv5s, there were cases where some of the power lines were not recognized and cases where non-power lines were incorrectly recognized as power lines. The SPLD recognizes continuous power lines as each area by connecting each point above and below the center points of the recognized bounding boxes. It recognized not only multiple power lines but also diagonal or curved power lines.

The performance of the SPLD was evaluated using the IoU and F1-score, which were 0.528 and 0.674, respectively. As a result of performing power line recognition under the same conditions using the U-Net, LaneNet and BiSeNet V2, the F1-score was 0.431, 0.465 and 0.663, and the IoU was 0.295, 0.309 and 0.507, respectively. The performance of the SPLD was better than those of the U-Net, LaneNet and BiSeNet V2. The U-net was weak in recognizing power lines in the background of mountains or fields, and the LaneNet recognized power lines as too thick, and BiSeNet V2 performed well in recognizing power lines overall, but there were cases where it mistook ridge for power lines. The SPLD corrects detection errors when a part of the power line is not recognized or when a non-power line is incorrectly recognized as a power line. The SPLD can recognize the shape and location of multiple power lines, and provide information about the number of power lines in images. As the SPLD was developed based on YOLOv5s, it could operate even in low-end deep learning embedded systems. In this study, the SPLD was performed on a low-end deep learning embedded system, Jetson Nano, and this system was installed on a drone. Power line recognition tests were conducted in an indoor virtual environment and an outdoor paddy field. Through tests, it was confirmed that power line recognition using the SPLD could be performed in real-time using embedded systems. The average FPS was 10.05. The FOV of the used camera,  $69^\circ \times 42^\circ$  (V×H), can capture all power lines in the drone's flight path. The limitation of this technology is that two or more adjacent power lines are recognized as one power line when they are located within 10 pixels based on the y-axis pixel. Future tasks will include developing technologies to distinguish adjacent power lines within 10 pixels, to recognize power lines even in low-visibility situations, and to measure the distance between a drone and power lines. This technology is expected to be used for safe flight of agricultural drones to prevent power line collisions and in fields requiring power line recognition, such as transmission line inspection and drone reconnaissance. The STRNet [24] and SDDNet [25] models used deep learning techniques to segment concrete crack images in real-time under complex backgrounds, and were tested on a GPU environment. It is expected that SPLD can be used to segment concrete cracks in real-time on embedded computers. This technology could also be applied to fields that require the recognition of thin and long objects, such as electric poles and parking lines.

## REFERENCES

- [1] A. Romero-Lugo, A. Magadan-Salazar, J. Fuentes-Pacheco, and R. Pinto-Eliás, "A comparison of deep neural networks for monocular depth map estimation in natural environments flying at low altitude," *Sensors*, vol. 22, no. 24, p. 9830, Dec. 2022, doi: [10.3390/s22249830](https://doi.org/10.3390/s22249830).
- [2] S. Back, G. Cho, J. Oh, X.-T. Tran, and H. Oh, "Autonomous UAV trail navigation with obstacle avoidance using deep neural networks," *J. Intell., Robot. Syst.*, vol. 100, nos. 3–4, pp. 1195–1211, Sep. 2020, doi: [10.1007/s10846-020-01254-5](https://doi.org/10.1007/s10846-020-01254-5).
- [3] J. Zhang, H. Sheng, Q. Chen, H. Zhou, B. Yin, J. Li, and M. Li, "A four-dimensional space-time automatic obstacle avoidance trajectory planning method for multi-UAV cooperative formation flight," *Drones*, vol. 6, no. 8, p. 192, Jul. 2022, doi: [10.3390/drones6080192](https://doi.org/10.3390/drones6080192).
- [4] Z. Li, Y. Liu, R. Walker, R. Hayward, and J. Zhang, "Towards automatic power line detection for a UAV surveillance system using pulse coupled neural filter and an improved Hough transform," *Mach. Vis. Appl.*, vol. 21, no. 5, pp. 677–686, Sep. 2009, doi: [10.1007/s00138-009-0206-y](https://doi.org/10.1007/s00138-009-0206-y).
- [5] M. H. Nasseri, H. Moradi, S. M. Nasiri, and R. Hosseini, "Power line detection and tracking using Hough transform and particle filter," in *Proc. 6th RSI Int. Conf. Robot. Mechatronics (ICRoM)*, Tehran, Iran, Oct. 2018, pp. 130–134, doi: [10.1109/ICRoM.2018.8657568](https://doi.org/10.1109/ICRoM.2018.8657568).
- [6] L. Baker, S. Mills, T. Langlotz, and C. Rathbone, "Power line detection using Hough transform and line tracing techniques," in *Proc. Int. Conf. Image Vis. Comput. New Zealand (IVCNZ)*, Palmerston North, New Zealand, Nov. 2016, pp. 1–6, doi: [10.1109/IVCNZ.2016.7804438](https://doi.org/10.1109/IVCNZ.2016.7804438).
- [7] V. N. Nguyen, R. Jenssen, and D. Roverso, "LS-Net: Fast single-shot line-segment detector," *Mach. Vis. Appl.*, vol. 32, no. 1, pp. 1–16, Oct. 2020, doi: [10.1007/s00138-020-01138-6](https://doi.org/10.1007/s00138-020-01138-6).
- [8] M. Hota, S. Rao B, and U. Kumar, "Power lines detection and segmentation in multi-spectral UAV images using convolutional neural network," in *Proc. IEEE India Geosci. Remote Sens. Symp. (InGARSS)*, Ahmedabad, India, Dec. 2020, pp. 154–157, doi: [10.1109/InGARSS48198.2020.9358967](https://doi.org/10.1109/InGARSS48198.2020.9358967).
- [9] K. Zhu, C. Xu, Y. Wei, and G. Cai, "Fast-PLDN: Fast power line detection network," *J. Real-Time Image Process.*, vol. 19, no. 1, pp. 3–13, Jul. 2021, doi: [10.1007/s11554-021-01154-3](https://doi.org/10.1007/s11554-021-01154-3).
- [10] H.-S. Son, D.-K. Kim, S.-H. Yang, and Y.-K. Choi, "Real-time power line detection for safe flight of agricultural spraying drones using embedded systems and deep learning," *IEEE Access*, vol. 10, pp. 54947–54956, 2022, doi: [10.1109/ACCESS.2022.3177196](https://doi.org/10.1109/ACCESS.2022.3177196).
- [11] Ultralytics. YOLOv5. Accessed: Jan. 5, 2023. [Online]. Available: <https://github.com/ultralytics/yolov5>
- [12] J. Yao, J. Qi, J. Zhang, H. Shao, J. Yang, and X. Li, "A real-time detection algorithm for kiwifruit defects based on YOLOv5," *Electronics*, vol. 10, no. 14, p. 1711, Jul. 2021, doi: [10.3390/electronics10141711](https://doi.org/10.3390/electronics10141711).
- [13] L. Zhu, X. Geng, Z. Li, and C. Liu, "Improving YOLOv5 with attention mechanism for detecting boulders from planetary images," *Remote Sens.*, vol. 13, no. 18, p. 3776, Sep. 2021, doi: [10.3390/rs13183776](https://doi.org/10.3390/rs13183776).
- [14] G. Lin, K. Liu, X. Xia, and R. Yan, "An efficient and intelligent detection method for fabric defects based on improved YOLOv5," *Sensors*, vol. 23, no. 1, p. 97, Dec. 2022, doi: [10.3390/s23010097](https://doi.org/10.3390/s23010097).
- [15] D. Neven, B. D. Brabandere, S. Georgoulis, M. Proesmans, and L. V. Gool, "Towards end-to-end lane detection: An instance segmentation approach," in *Proc. IEEE Intell. Vehicles Symp. (IV)*, Changshu, China, Jun. 2018, pp. 286–291, doi: [10.1109/IVS.2018.8500547](https://doi.org/10.1109/IVS.2018.8500547).
- [16] Z. Wang, W. Ren, and Q. Qiu, "LaneNet: Real-time lane detection networks for autonomous driving," 2018, *arXiv:1807.01726*.
- [17] S. M. Azimi, P. Fischer, M. Körner, and P. Reinartz, "Aerial LaneNet: Lane-marking semantic segmentation in aerial imagery using wavelet-enhanced cost-sensitive symmetric fully convolutional neural networks," *IEEE Trans. Geosci. Remote Sens.*, vol. 57, no. 5, pp. 2920–2938, May 2019, doi: [10.1109/TGRS.2018.2878510](https://doi.org/10.1109/TGRS.2018.2878510).
- [18] L.-A. Tran and M.-H. Le, "Robust U-Net-based road lane markings detection for autonomous driving," in *Proc. Int. Conf. Syst. Sci. Eng. (ICSSE)*, Dong Hoi, Vietnam, Jul. 2019, pp. 62–66, doi: [10.1109/ICSSE.2019.8823532](https://doi.org/10.1109/ICSSE.2019.8823532).
- [19] B. C. Choi, J. Kwon, and H. Nam, "Image prediction for lane following assist using convolutional neural network-based U-Net," in *Proc. Int. Conf. Artif. Intell. Inf. Commun. (ICAIIIC)*, Jeju Island, Republic of Korea, Feb. 2022, pp. 78–81, doi: [10.1109/ICAIIIC54071.2022.9722658](https://doi.org/10.1109/ICAIIIC54071.2022.9722658).
- [20] Z. Zhang, Q. Liu, and Y. Wang, "Road extraction by deep residual U-Net," *IEEE Geosci. Remote Sens. Lett.*, vol. 15, no. 5, pp. 749–753, May 2018, doi: [10.1109/LGRS.2018.2802944](https://doi.org/10.1109/LGRS.2018.2802944).

- [21] N. Y. Q. Abderrahim, S. Abderrahim, and A. Rida, "Road segmentation using U-Net architecture," in *Proc. IEEE Int. Conf. Moroccan Geomatics (Morgeo)*, Casablanca, Morocco, May 2020, pp. 1–4, doi: [10.1109/Morgeo49228.2020.9121887](https://doi.org/10.1109/Morgeo49228.2020.9121887).
- [22] C. Yu, C. Gao, J. Wang, G. Yu, C. Shen, and N. Sang, "BiSeNet V2: Bilateral network with guided aggregation for real-time semantic segmentation," 2020, *arXiv:2004.02147*.
- [23] R. Dong, X. Pan, and F. Li, "DenseU-Net-based semantic segmentation of small objects in urban remote sensing images," *IEEE Access*, vol. 7, pp. 65347–65356, 2019, doi: [10.1109/ACCESS.2019.2917952](https://doi.org/10.1109/ACCESS.2019.2917952).
- [24] D. H. Kang and Y.-J. Cha, "Efficient attention-based deep encoder and decoder for automatic crack segmentation," *Struct. Health Monitor.*, vol. 21, no. 5, pp. 2190–2205, Sep. 2022, doi: [10.1177/14759217211053776](https://doi.org/10.1177/14759217211053776).
- [25] W. Choi and Y.-J. Cha, "SDDNet: Real-time crack segmentation," *IEEE Trans. Ind. Electron.*, vol. 67, no. 9, pp. 8016–8025, Sep. 2020, doi: [10.1109/TIE.2019.2945265](https://doi.org/10.1109/TIE.2019.2945265).



**HYUN-SIK SON** was born in Ulsan, Republic of Korea, in 1989. He received the B.S. and M.S. degrees from the Department of Electrical and Electronic Engineering, Pusan National University, in 2015 and 2017, respectively. He is currently pursuing the Ph.D. degree with the Department of Electrical and Computer Engineering, Pusan National University.

Since 2017, he has been a Research Assistant with the Smart Agricultural Machinery Research and Development Group, Korea Institute of Industrial Technology. His research interests include artificial intelligence, autonomous driving, and deep learning.



**DEOK-KEUN KIM** received the B.S. and M.S. degrees in biosystem engineering from Chonnam National University, Gwangju, South Korea, in 2016 and 2019, respectively, where he is currently pursuing the Ph.D. degree with the Interdisciplinary Program in Agricultural and Life Science.

Since 2005, he has been a Research Assistant with the Smart Agricultural Machinery Research and Development Group, Korea Institute of Industrial Technology. His research interests include the development of the smart farm, agricultural robots, and precision agriculture.



**SEUNG-HWAN YANG** was born in Seoul, Republic of Korea, in 1979. He received the B.S. degree in agricultural machinery engineering and the M.S. and Ph.D. degrees in biosystems engineering from Seoul National University, in 2002, 2007, and 2011, respectively.

From 2002 to 2005, he was a Computer Programmer with IBK System and Syswill. From 2011 to 2013, he was a Postdoctoral Researcher with the Korea Research Institute of Standards and Science. Since 2013, he has been a Principal Researcher with the Smart Agricultural Machinery Research and Development Group, Korea Institute of Industrial Technology. He has participated in more than 40 research projects. He is the author of more than ten articles. He holds more than 20 patents. His research interests include agricultural automation and robotics using the IoT, ICT, and AI technology.



**YOUNG-KIU CHOI** received the B.S. degree in electrical engineering from Seoul National University, Seoul, South Korea, in 1980, and the M.S. and Ph.D. degrees in electrical engineering from the Korea Advanced Institute of Science and Technology (KAIST), Seoul, in 1982 and 1987, respectively.

Since 1986, he has been a Professor with the Department of Electrical and Computer Engineering, Pusan National University, Pusan, South Korea. He was a Visiting Scholar with the California Institute of Technology, Pasadena, CA, USA, from 1990 to 1991, and a Visiting Professor with the University of Southwestern Louisiana, Lafayette, LA, USA, from 1998 to 1999. His research interests include intelligent control, evolutionary algorithms, variable-structure control, robotics, and power electronics.

...